APPLIED MATHEMATICS

Stochastic Modelling of Early-Life Stress and Long-Term Psychological Well-Being: Thresholds in a Shot-Noise Model of Allostatic Load

Andanje Mulambula

Department of Mathematics, Kibabii University, Bungoma, Kenya

Published November 2026

Abstract

Early-life stress is reliably associated with poorer psychological well-being decades later, but the mechanism by which an exposure that ends in childhood continues to act in adulthood is not settled. This paper formalises the question as a problem in stochastic processes. Allostatic load is modelled as a shot-noise process driven by a Poisson stream of stressors with exponentially distributed magnitudes and a homeostatic recovery rate. Two results follow. First, in the constant-parameter model the influence of a childhood stressor on adult load decays exponentially and is numerically extinct within a decade, so the state variable cannot carry the observed persistence; persistence must instead enter through a parameter. Second, when childhood exposure is allowed to lower the recovery rate, the stationary load distribution is exactly Gamma with shape equal to the ratio of the stressor arrival rate to the recovery rate, and two exposure thresholds appear in closed form. At the first, the modal load leaves zero and the typical state changes from recovered to elevated. At the second, located by a digamma equation, the rate of threshold crossings is maximised; beyond it episodes become fewer but longer, so disturbance shifts from episodic to chronic. The exceedance probability, episode rate and mean episode duration all have closed forms, each confirmed against exact simulation. The model further predicts that exposures of equal count but earlier timing carry greater adult risk, a prediction count-based epidemiology cannot test.

Keywords: Allostatic load; biological embedding; early-life stress; shot-noise process; stationary distribution; threshold behaviour

1 Introduction

Adults who report adverse experiences in childhood are, on average, in poorer psychological health than those who do not, and the association is graded: risk rises with the number of distinct adversities reported. The association is among the most reproducible in psychiatric epidemiology. Its mechanism is less settled. An exposure that ends at the age of eighteen is still associated with outcomes at fifty, and a satisfactory account must explain how a cause that has stopped acting continues to make a difference decades later.

This paper treats that question as a problem in stochastic processes rather than as a problem of measurement. The object modelled is allostatic load, the cumulative physiological cost of repeated activation of the stress response [3], a construct built on the notion of allostasis introduced by Sterling and Eyer [4]. Load is driven up by discrete stressors and falls back between them through homeostatic recovery. That description is already a stochastic process of a familiar kind, and writing it down exposes the difficulty precisely.

The difficulty is this. In a model where stressors arrive at a constant rate and recovery proceeds at a constant rate, the influence of any particular stressor on the state of the system decays exponentially. Section 3.1 makes the point quantitatively: with recovery rates in a plausible range, the direct contribution of a stressor experienced at age ten to the load carried at age fifty is of order ten to the minus nine. The state variable simply does not remember. Any model of this class that leaves its parameters fixed therefore predicts no long-term effect of early-life stress, whatever the size of the early exposure.

It follows that persistence has to be carried by a parameter rather than by the state. The parameter that the biology nominates is the recovery rate itself. Under the heading of biological embedding, a term introduced by Hertzman [5] and developed into a mechanistic model by Miller, Chen and Parker [6], early adversity is held to alter the regulatory set-up of the stress-response system in ways that outlast the exposure. In the present model that is represented in the simplest possible way: childhood exposure lowers the recovery rate, permanently.

Two things then follow, and both are exact. The stationary distribution of load is a Gamma law whose shape parameter is the ratio of the stressor arrival rate to the recovery rate. Because exposure enters only through that ratio, the long-run behaviour of the system is governed by a single dimensionless quantity, and the qualitative form of the distribution changes as that quantity passes one. Below the transition the modal load is zero and the typical state is a recovered one, punctuated by excursions. Above it the mode is interior and positive, and the typical state is an elevated one. The exposure at which this happens has a closed form.

A second threshold appears when one asks not how much load is carried but how it is distributed in time. The rate at which load crosses a fixed clinical threshold also has a closed form, and it is not monotone in exposure. It rises, peaks, and falls. The peak is located by a digamma equation. Beyond it, episodes become less frequent but substantially longer: the system stops oscillating in and out of the elevated region and begins to sit in it. In clinical language the model predicts a shift from episodic to chronic disturbance, and it predicts where that shift occurs.

The model sits alongside a small body of prior work. Benthem de Grave, Hasselman and Bijleveld [12] give a computational model of work stress in which discrete stressors arrive as a Poisson stream and the cortisol response decays exponentially, which is a shot-noise architecture of the same family as the one used here; their allostatic load accumulates irreversibly above a strain threshold and their outcome is disease onset. They do not identify a stationary law, and they hold the recovery coefficient fixed and identical across individuals, noting inter-individual variation in that coefficient as an open problem. The present paper takes up that problem and supplies the missing closed forms. Rao and Androulakis [13] model the hypothalamic–pituitary–adrenal axis as a deterministic oscillator and operationalise allostatic load as a contraction of the viable parameter space, with no stochastic forcing and no cumulative load variable. Van de Leemput and colleagues [14] provide the methodological precedent for treating resilience as a recovery rate and its loss as a reduction in that rate, by way of critical slowing down in intensive longitudinal mood data. Waugh and Sali [20] use the vocabulary of allostatic modelling but present no equations or parameters.

The contribution claimed here is correspondingly narrow. A Poisson-driven, exponentially-decaying model of allostatic load is not new. What appears to be new is the closed-form stationary characterisation of such a model, and the treatment of early adversity as acting on the recovery rate rather than on the state or the baseline, together with the threshold structure that follows from it.

The paper is organised as follows. Section 2 sets out the model. Section 3 derives the analytical results: the influence kernel, the stationary law, the two thresholds, and the episode statistics. Section 4 describes the numerical methods. Section 5 reports the numerical results and the validation of each closed form against exact simulation. Section 6 compares the model against published dose–response estimates, Section 7 discusses what the model does and does not establish, and Section 8 concludes. The limitations are stated in Section 7.3 rather than deferred, because several of them bear directly on how the results should be read.

2 The model

2.1 Allostatic load as a shot-noise process

Let $A(t)$ denote allostatic load at age t, a non-negative quantity measuring cumulative physiological wear. Load decays towards zero at rate ρ and is raised by discrete stressors:

$$dA(t) = -\rho A(t)dt + dJ(t),\ J(t) = \sum_{i:t_i \le t} Y_i \tag{1}$$

where the stressor times and magnitudes satisfy

$$\{t_i\} \sim \mathrm{PP}(\lambda),\ Y_i \tilde{iid} \mathrm{Exp}(\beta) \tag{2}$$

The arrival rate λ and the mean stressor magnitude $1/\beta$ describe the environment; the recovery rate ρ describes the individual. Solving the linear equation between jumps gives

$$A(t) = A(0)e^{-\rho t} + \int_0^t e^{-\rho(t-s)}dJ(s) \tag{3}$$

so the influence on the load at age t of a stressor experienced at age s is carried by the kernel

$$\mathcal{K}(s,\ t) = \exp\left(-\int_s^t \rho(u)du\right) \tag{4}$$

which is the quantity Section 3.1 examines. The process is non-negative by construction, since both the initial condition and every increment are non-negative and decay preserves sign. This is a desirable property for a model of physiological wear and it is one reason for preferring a jump-driven formulation to an additive Gaussian one, which would place positive probability on negative load.

2.2 Biological embedding of the recovery rate

Childhood exposure is represented by a dose D accumulated over a developmental window, which acts on the recovery rate multiplicatively:

$$\rho(D) = \rho_0 e^{-D} \tag{5}$$

with ρ_0 the recovery rate of an unexposed individual. The exponential form is chosen for three reasons: it keeps the recovery rate positive for every dose, it makes the effect of successive adversities multiplicative rather than additive, which matches the approximately log-linear dose-response reported in the epidemiological literature, and it yields closed forms throughout. It is a modelling choice and not a derived law, and Section 7.3 returns to it.

The decision to locate the effect of early adversity in the recovery rate rather than in the baseline requires a candid statement of the evidence, because that evidence is weaker and more contested

than the modelling literature generally acknowledges. The direct support is narrow. Heim and colleagues [7] found greater escape from dexamethasone suppression in abused men, indicating less efficient glucocorticoid negative feedback, with a dose-response in the number of abuse events and in earlier onset. Converging indirect support comes from diurnal data: Marques-Feixa and colleagues [10] report a less pronounced evening decline and elevated bedtime cortisol in maltreated children and adolescents, in a dose-response with severity and frequency, and the meta-analysis of Perrone and colleagues [11] finds elevated bedtime cortisol to be the one significant diurnal effect among those examined.

Against this, three qualifications must be entered. First, the dominant meta-analytic finding in this literature is blunted reactivity rather than impaired recovery: Bunea and colleagues [9] report a reduced cortisol response to social stress at every phase measured, and their recovery outcome is a cortisol level sixty minutes after the stressor rather than a rate, and is lower in the exposed group. That result cannot be read as support for slower recovery, and if anything it argues for reducing the input gain instead. Second, the direct feedback evidence is contradictory: Newport and colleagues [8], working in the same research group as [7], found enhanced rather than reduced feedback in depressed abuse survivors, and concluded that the direction of the change tracks the resulting psychiatric illness rather than the exposure itself. Third, the diurnal effects reported in [11] are small and largely null outside the bedtime measure.

The reduced-recovery-rate parameterisation is therefore adopted here as a modelling choice worth exploring and not as an established mechanism. Its strongest justification is methodological rather than endocrinological: it follows the precedent of [14], in which resilience is operationalised as a recovery rate and loss of resilience as a reduction in that rate. A reader who rejects the parameterisation should note that the negative result of Section 3.1 stands regardless, and that it requires some parameter to carry the persistence even if not this one.

The dose itself accumulates over childhood, weighted by an age-dependent sensitivity:

$$D = \sum_{j:u_j \le \tau} \kappa\left(u_j\right) Y_j, \; \kappa(u) = \kappa_0 e^{-u/u_s} \tag{6}$$

so that a stressor of given magnitude contributes more to the permanent reduction in recovery capacity the earlier it is experienced. The sensitivity scale u_s sets the width of the developmental window. Taking expectations over the timing and magnitude of a given number of childhood stressors E gives

$$\mathbb{E}[D|E] = \kappa E, \; \kappa = \kappa_0 \bar{u}/\beta \tag{7}$$

which defines the single embedding coefficient κ used in the closed-form results. Where the paper writes results in terms of an exposure count E, that count is to be read as the age-averaged exposure; Section 5.4 treats timing explicitly and shows that the averaging discards information.

2.3 Well-being and the clinical threshold

Two readings of psychological well-being are used. The first is a monotone decreasing transform of load,

$$W(t) = \frac{W_{\max}}{1 + \left(A(t)/A_{50}\right)^{n_H}} \tag{8}$$

which is convenient for describing graded outcomes but introduces three further parameters. The second, used throughout the analytical results, is a threshold reading: load above a level θ is taken to index a clinically significant state. The threshold reading is preferred here because it requires one parameter rather than three, because it is what case-definition in psychiatric epidemiology actually does, and because it is the reading under which the model yields exact results. Nothing in Sections 3 to 5 depends on the Hill form.

3 Analytical results

3.1 The state cannot carry persistence

With ρ constant the influence kernel is $e^{-\rho(t-s)}$, so that

$$\lim_{t\to\infty} \mathcal{K}(s,\ t) = 0 \ \text{ for every fixed } s \tag{9}$$

The decay is not merely asymptotic but fast on the timescale of a human life. For recovery rates of 0.5, 1 and 2 per year the kernel at a lag of forty years takes the values 2.1×10^{-9}, 4.3×10^{-18} and 1.8×10^{-35} respectively. A model of this class with fixed parameters predicts that the adult load of an individual exposed in childhood is statistically indistinguishable from that of an individual who was not, however severe the childhood exposure.

This is worth stating as a negative result, because it constrains the class of admissible explanations rather than merely motivating one. Any stochastic model in which early adversity acts only on the state, and in which the dynamics are otherwise stationary, is incompatible with the observed persistence of early-life stress effects. Persistence must be carried by a parameter of the process. The remainder of the paper explores the consequences of locating it in the recovery rate, which is the choice the biology suggests, but the negative result is independent of that particular choice.

3.2 The stationary distribution

For constant ρ and λ the process is positive recurrent and its stationary law is available in closed form. The stationary variable is the stochastic integral of the decaying kernel against the jump measure, and its Laplace transform follows from the Lévy–Khintchine representation as

$$\mathbb{E}\left[e^{-\vartheta A_\infty}\right] = \left(1 + \vartheta/\beta\right)^{-\lambda/\rho} \tag{10}$$

which is the transform of a Gamma law. Writing $k = \lambda/\rho$,

$$A_\infty \sim \Gamma\left(k,\ \beta\right),\ k = \frac{\lambda}{\rho} \tag{11}$$

The result is classical for shot noise with exponential marks; see Bondesson [15, ch. 10] and, in precisely the present notation, Iksanov and Jurek [16]. It is also the stationary law of the Gamma Ornstein–Uhlenbeck process in the non-Gaussian Ornstein–Uhlenbeck framework of Barndorff-Nielsen and Shephard [17]. The density is

$$f(a) = \frac{\beta^k a^{k-1} e^{-\beta a}}{\Gamma(k)},\ a > 0 \tag{12}$$

and moments

$$\mathbb{E}\left[A_\infty\right] = \frac{k}{\beta} = \frac{\lambda}{\rho\beta},\ \operatorname{Var}\left[A_\infty\right] = \frac{k}{\beta^2} \tag{13}$$

The shape parameter k is the ratio of the rate at which the environment delivers stressors to the rate at which the individual clears them, and it is the only quantity through which either enters the stationary law. Two individuals with different arrival and recovery rates but the same ratio have identical long-run load distributions. The scale is set by β alone.

3.3 The first threshold: The typical state

The Gamma density is monotone decreasing when the shape parameter is at most one and unimodal with an interior maximum when it exceeds one:

$$\operatorname{mode}(A_\infty) = \begin{cases} 0, & k \le 1, \\ (k-1)/\beta, & k > 1. \end{cases} \tag{14}$$

The transition at $k = 1$ is a change in the qualitative form of the distribution, not merely in its location. Below it the single most likely state is full recovery and elevated load is an excursion; above it the single most likely state is elevated and full recovery is the excursion. Substituting the embedded recovery rate and solving for the exposure at which $k = 1$ gives

$$E^* = \frac{1}{\kappa} \ln \frac{\rho_0}{\lambda} \tag{15}$$

With the parameters used throughout this paper ($\rho_0 = 2.0$, $\lambda = 1.0$, $\kappa = 0.25$) the critical exposure is $E^* = 2.773$. The threshold depends on the environment only through the ratio ρ_0/λ, so an individual in a harsher adult environment reaches it after less childhood exposure.

The probability that load exceeds a clinical threshold follows from the same law:

$$P(A_\infty > \theta) = Q(k, \beta\theta) = \frac{\Gamma(k, \beta\theta)}{\Gamma(k)} \tag{16}$$

with Q the regularised upper incomplete gamma function.

3.4 Episodes: Rate and duration

Prevalence alone does not distinguish an individual with frequent brief disturbances from one with rare prolonged disturbances, and the distinction is clinically material. Because load decreases continuously between stressors and increases only at them, upcrossings of the level θ occur only at arrival times. By the PASTA property the pre-jump state is distributed according to the stationary law, so the upcrossing rate is

$$\nu(\theta) = \lambda \int_0^\theta f(a) e^{-\beta(\theta - a)} da \tag{17}$$

and the integral evaluates in closed form:

$$\nu(\theta) = \lambda \frac{e^{-\beta\theta} (\beta\theta)^k}{\Gamma(k+1)} \tag{18}$$

Combining with the exceedance probability and the ergodic identity that the long-run fraction of time above θ equals the product of the episode rate and the mean episode length gives

$$\overline{T}(\theta) = \frac{P(A_\infty > \theta)}{\nu(\theta)} = \frac{Q(k, \beta\theta)\Gamma(k+1)}{\lambda e^{-\beta\theta} (\beta\theta)^k} \tag{19}$$

The two expressions together characterise the temporal structure of the disturbance: how often it starts, and how long it lasts once started. Neither is available from the exceedance probability alone.

Two remarks on the episode rate are worth recording. It admits the equivalent form

$$\nu(\theta) = \lambda\left[Q(k+1,\ \beta\theta) - Q(k,\ \beta\theta)\right] \tag{20}$$

so that ν/λ is the difference of two incomplete gamma functions and, for integer k, is exactly the Poisson probability of observing k events with mean βθ. The three routes to ν — the integral above, this identity, and direct simulation — agree to within one part in ten million. And ν should not be read as a rate of exceedance: it counts upward crossings, so it vanishes as θ tends to zero, because the stationary load is almost surely positive and the process is then already above the level rather than crossing it. As a function of θ it rises from zero, peaks at βθ = k, and decays.

3.5 The second threshold: Episodic to chronic

The episode rate is not monotone in exposure. Differentiating the logarithm of the rate with respect to the shape parameter and setting the result to zero gives the stationary condition

$$\psi(k_{\max} + 1) = \ln(\beta\theta) \tag{21}$$

where ψ is the digamma function. Since $\psi(k+1)$ increases strictly from $-\gamma$ to infinity on $k > 0$, this equation has a positive root if and only if

$$\beta\theta > e^{-\gamma} \approx 0.5615 \tag{22}$$

with γ the Euler–Mascheroni constant. When that condition fails the derivative is negative throughout, the episode rate decreases monotonically in exposure, and there is no interior maximum; the supremum is then the boundary value $\lambda e^{-\beta\theta}$ approached as k tends to zero. The condition is mild — it fails only for thresholds below about 0.56 times the mean stressor magnitude, which is well inside the range of ordinary fluctuation and would not be used as a clinical threshold — but the second threshold is not unconditional and the statement below assumes it holds. For the parameters of this paper βθ = 3.

Where the condition does hold, the corresponding exposure is

$$E_{\max} = \frac{1}{\kappa} \ln \frac{k_{\max}\rho_0}{\lambda} \tag{23}$$

With the parameters of this paper, $k_{\max}$ = 2.4863 and $E_{\max}$ = 6.416. Below $E_{\max}$ further exposure makes episodes more frequent; above it, further exposure makes them less frequent but longer, because the process increasingly fails to return below the threshold between stressors. The exceedance probability continues to rise throughout, so the decline in episode rate is not a decline in burden. It is a change in the form the burden takes.

This is the model's sharpest clinical prediction, and it is one that prevalence-based epidemiology cannot see. Two populations with the same point prevalence of elevated load may differ substantially in whether that prevalence is composed of many short episodes or few long ones, and the model says which to expect from the exposure history.

3.6 The elasticity of load to exposure

Under embedding the stationary mean load is

$$\mathbb{E}\left[A_\infty | E\right] = \frac{\lambda}{\rho_0 \beta} e^{\kappa E} \tag{24}$$

so that

$$\frac{\partial}{\partial E}\mathbb{E}\left[A_\infty | E\right] = \kappa \mathbb{E}\left[A_\infty | E\right] \tag{25}$$

The proportional effect of an additional unit of childhood exposure on mean adult load is constant, which is to say the absolute effect grows with the exposure already sustained. This is the model's formal counterpart of the graded dose-response reported in the epidemiological literature, and it arises from the multiplicative form of the embedding rather than being imposed separately.

4 Numerical methods

The shot-noise process is simulated exactly rather than by discretisation. Between arrivals the trajectory is deterministic, so the state immediately after the ith arrival is the previous state multiplied by $e^{-\rho \Delta t}$ plus an exponential draw, where Δt is an exponential inter-arrival time. No time-stepping error is incurred and the only error is Monte Carlo. Stationary samples are drawn by reading one long trajectory at equally spaced times after a burn-in of one hundred years.

Episode statistics are accumulated along the same trajectories. Upcrossings are counted at arrival times by comparing the pre-jump and post-jump states against the threshold; time above the threshold is accumulated in closed form over each decay segment, since the time spent above a level while decaying exponentially from a known value is available analytically. This avoids the discretisation bias that a fixed time grid would introduce into both quantities.

The robustness calculations of Section 5.4 add a diffusion term and therefore require discretisation. A Cox–Ingersoll–Ross form is used,

$$dA(t) = -\rho A(t) dt + \sigma \sqrt{A(t)} dW(t) + dJ(t) \tag{26}$$

with full truncation at zero, integrated by Euler–Maruyama at a step of 2×10^{-3} years. The square-root coefficient is chosen so that the diffusion vanishes at the origin and the process remains non-negative, which an additive Gaussian term would not.

All reported figures are reproducible from the accompanying implementation with the seeds stated there. Convergence of the Monte Carlo estimates against their exact values is reported in Table 6.

5 Results

5.1 Validation of the stationary law

Table 1 compares the simulated stationary moments against the Gamma law across five parameter combinations spanning shape parameters from 0.2 to 5. Agreement is to three decimal places in the mean and to two in the variance, and a Kolmogorov–Smirnov test against the predicted law is non-significant in every case.

Table 1. Stationary law against exact simulation.

λ, ρ	k	mean sim	mean thy	var sim	var thy	KS p
1.0, 2.0	0.50	0.496	0.500	0.483	0.500	0.827
2.0, 1.0	2.00	2.004	2.000	1.988	2.000	0.362
3.0, 1.5	2.00	2.004	2.000	2.020	2.000	0.748
0.8, 4.0	0.20	0.199	0.200	0.194	0.200	0.146
5.0, 1.0	5.00	4.988	5.000	4.881	5.000	0.345

Figure 1 shows the simulated stationary load against the predicted Gamma density, for shape parameters below and above the transition at one.

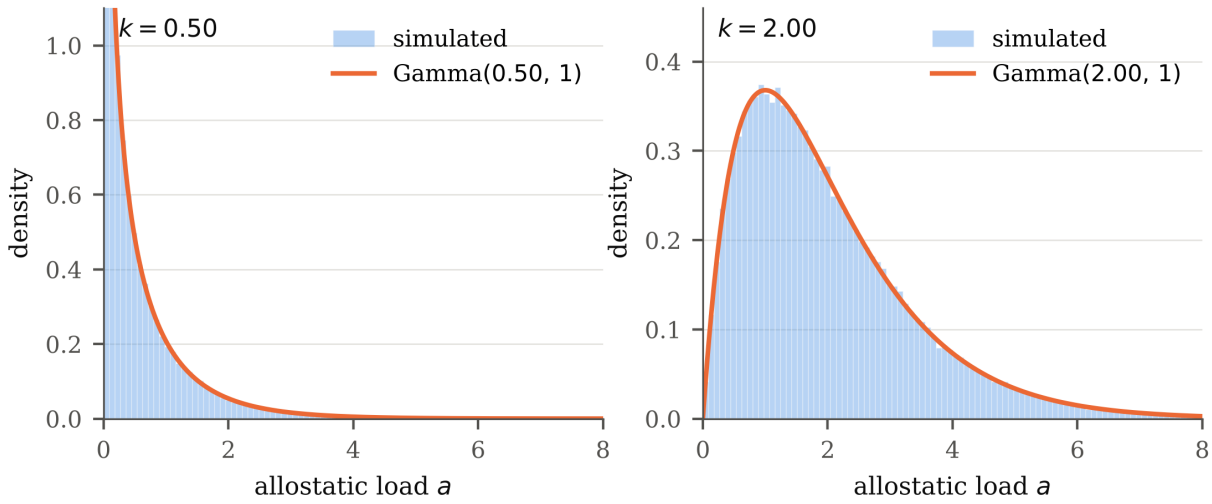


Figure 1. Simulated stationary load against the predicted Gamma density, for shape parameters below and above the transition at one. Upper panel k = 0.50; lower panel k = 2.00. Histograms from 120,000 stationary samples.

5.2 The two thresholds

Table 2 traces the exposure gradient through both thresholds. The modal load leaves zero at E^*; the episode rate peaks at $E_{\max}$ and declines thereafter while the mean episode duration continues to rise.

Table 2. The exposure gradient and the two thresholds.

E	ρ(E)	k	mode	P(A>θ)	ν (yr^{-1})	dur (yr)
0.00	2.000	0.500	0.000	0.0143	0.0973	0.147
1.00	1.558	0.642	0.000	0.0219	0.1121	0.195
2.00	1.213	0.824	0.000	0.0345	0.1313	0.263
2.77	1.000	1.000	0.000	0.0498	0.1494	0.333
4.00	0.736	1.359	0.359	0.0915	0.1832	0.499
6.42	0.402	2.486	1.486	0.3031	0.2335	1.298
8.00	0.271	3.695	2.695	0.5830	0.1883	3.096

Figure 2 shows the stationary load densities across the exposure gradient.

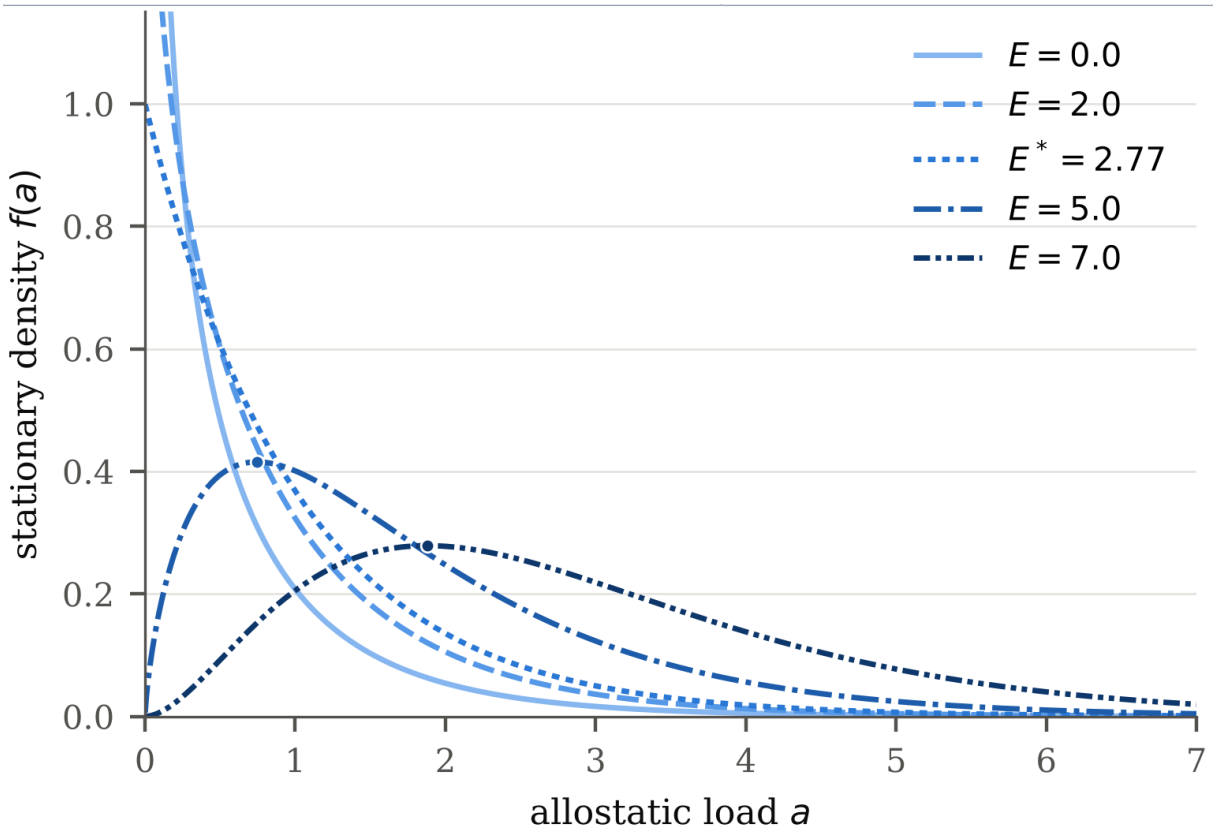


Figure 2. Stationary load densities across the exposure gradient. The mode leaves the origin as the exposure passes E; filled markers show the interior modes.

Figure 3 shows the exceedance probability, episode rate and mean episode duration against childhood exposure.

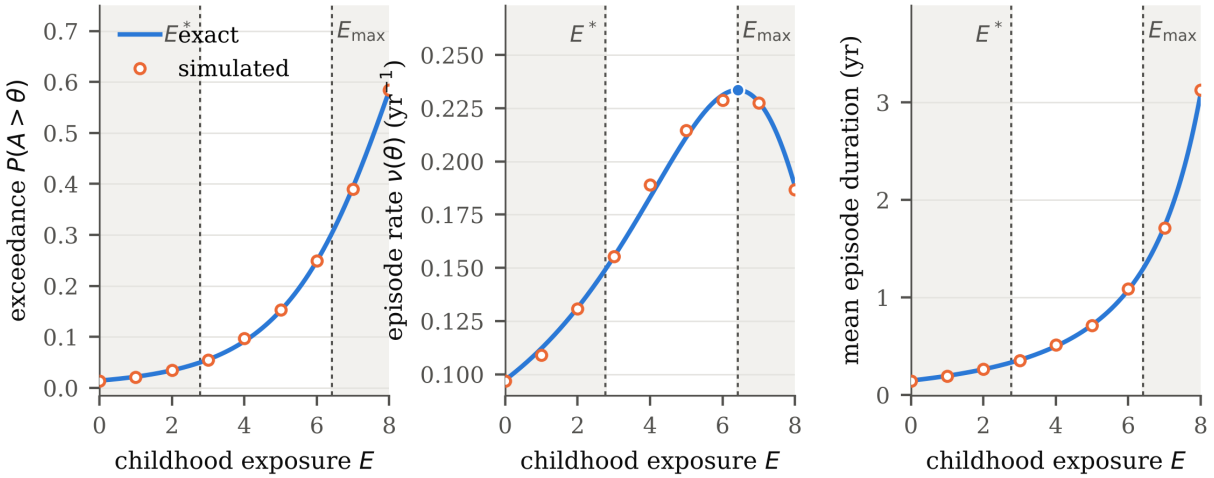


Figure 3. Exceedance probability, episode rate and mean episode duration against childhood exposure. Curves are the closed forms; circles are exact simulation. Shaded regions lie outside the two thresholds. The episode rate peaks at Emax, marked by the filled point.

5.3 Episode statistics

Table 3 validates the closed forms for the episode rate and the mean episode duration against simulation over 200,000 years of trajectory per parameter set, across thresholds and shape parameters.

Table 3. Episode rate and duration against simulation.

λ, ρ, θ	k	v thy	v sim	dur thy	dur sim
1.0, 2.0, 3	0.50	0.09730	0.09649	0.1470	0.1455
1.0, 1.0, 3	1.00	0.14936	0.15033	0.3333	0.3286
2.0, 1.0, 3	2.00	0.44808	0.45082	0.4444	0.4432
1.0, 1.0, 2	1.00	0.27067	0.27223	0.5000	0.4986
1.0, 0.6, 4	1.67	0.12270	0.12327	0.4816	0.4760

Figure 4 shows the adult load trajectories over sixty years at three exposure levels, with the clinical threshold marked.

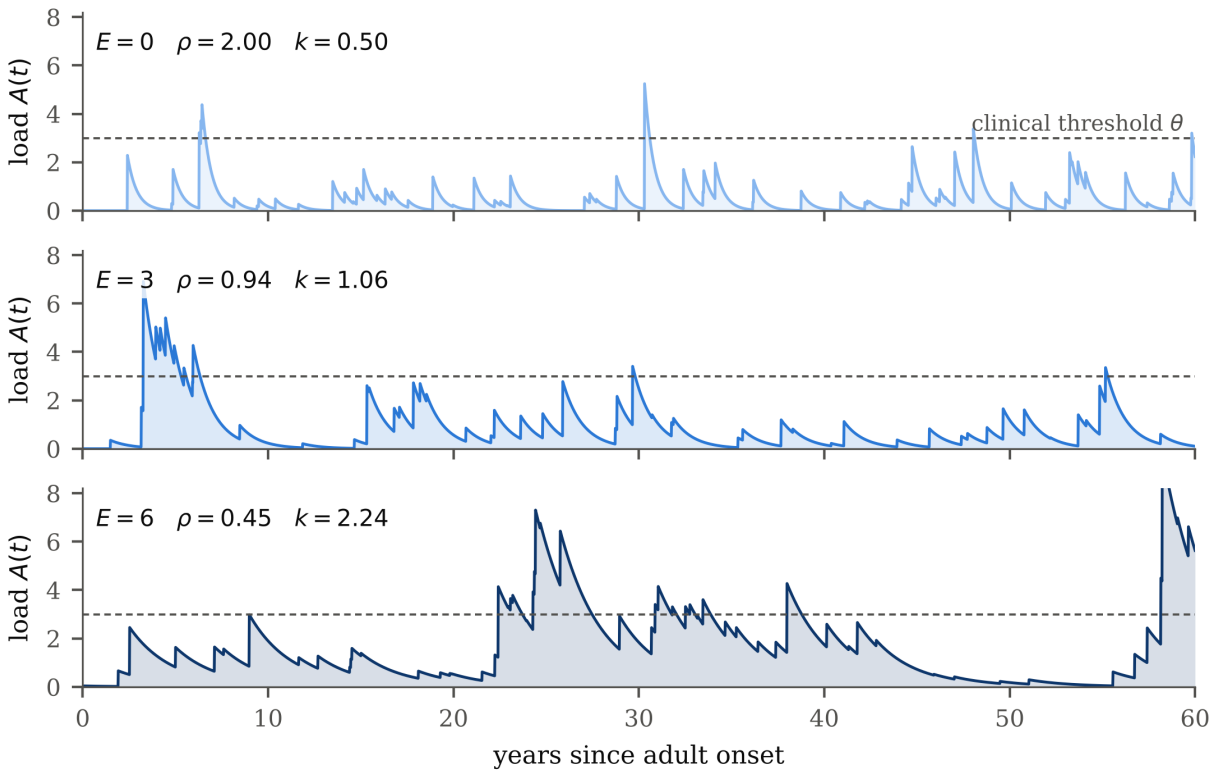


Figure 4. Adult load trajectories over sixty years at three exposure levels, with the clinical threshold marked. The same stressor environment produces isolated excursions at E = 0, longer excursions at E = 3, and sustained elevation at E = 6.

5.4 Sensitive periods

Because the embedding weight declines with age, two individuals with the same number of childhood stressors but different timing acquire different adult risk. Table 4 shows this for two stressors of equal magnitude placed at different ages; the ratio of adult exceedance probabilities between the earliest and latest placements is 1.97. The last row shows that a widely spaced pair is not equivalent to either a concentrated early pair or a concentrated late one.

Table 4. Equal exposure count, different timing.

ages (yr)	dose	ρ	k	P(A>θ)
1, 3	0.4359	1.2934	0.773	0.0306

ages (yr)	dose	ρ	k	P(A>θ)
3, 5	0.3123	1.4635	0.683	0.0245
8, 10	0.1357	1.7461	0.573	0.0180
14, 16	0.0499	1.9026	0.526	0.0155
1, 16	0.2748	1.5195	0.658	0.0229

Figure 5 shows the adult exceedance probability against the age at which a single stressor is experienced, for three stressor severities.

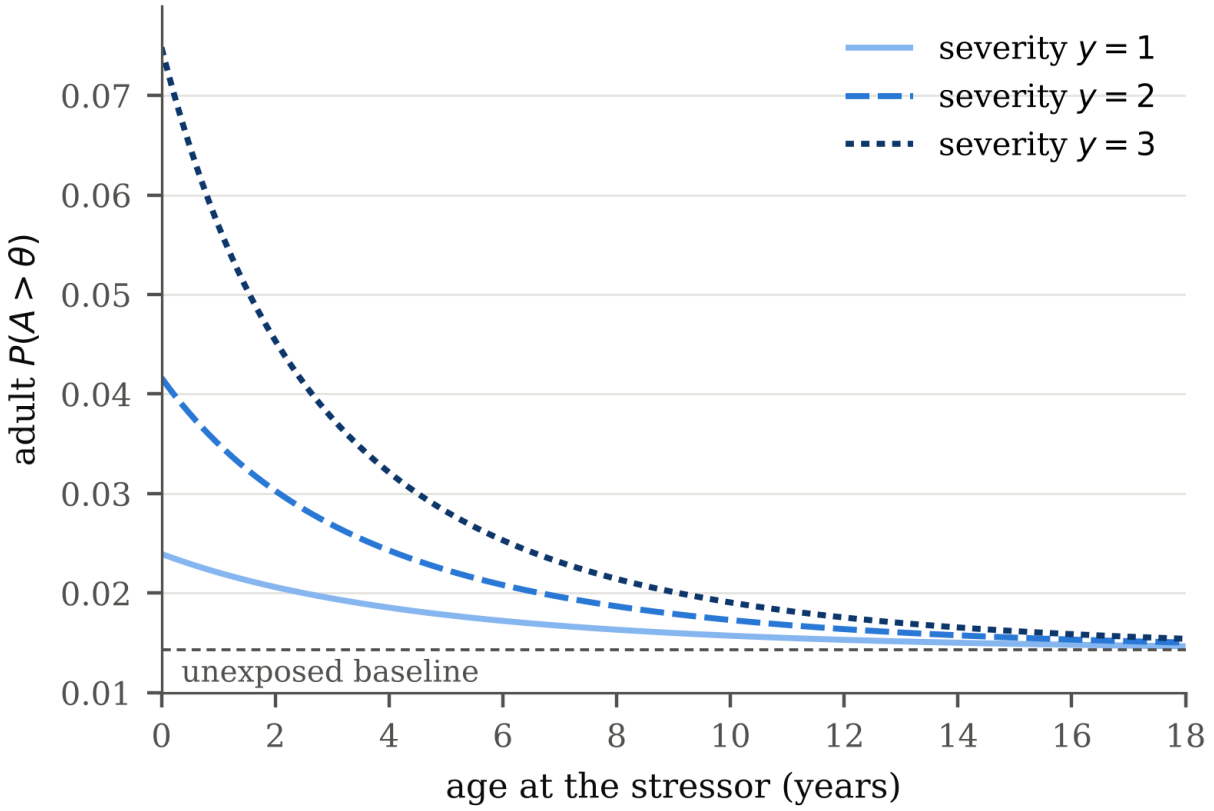


Figure 5. Adult exceedance probability against the age at which a single stressor is experienced, for three stressor severities. Risk converges on the unexposed baseline as the age at exposure increases.

This is a testable prediction and a point of leverage against the epidemiological literature, which codes adversity predominantly as a count. Under the model, count-based measures are a lossy summary of exposure history, and two cohorts matched on count but differing in timing should show systematically different adult risk. The model also implies that the loss is not symmetric: misdating an early exposure as late understates risk by more than the converse overstates it, because the weight function is convex over the range where most exposure occurs.

5.5 Robustness to within-day variability

Table 5 repeats the exposure gradient with a diffusion term added. The gradient is preserved at every noise level. The largest shift relative to the pure jump model is 3.6 percentage points, at the strongest noise and the highest exposure; below that the shifts are under one point at the weakest noise and under three at intermediate noise. The qualitative conclusions therefore do not rest on the absence of continuous variability, though the quantitative values do move.

Table 5. Exceedance probability with added diffusion.

σ	E = 0	E = 2	E = 4	E = 6
0.0	0.0141	0.0340	0.0917	0.2509
0.3	0.0115	0.0377	0.0954	0.2606
0.6	0.0171	0.0420	0.0975	0.2780
1.0	0.0180	0.0545	0.1225	0.2873

The exact Gamma law is a property of the pure jump model and is lost once the diffusion is added, which is the price of the generalisation. What Table 5 establishes is that the dose-response and the ordering of the regimes survive it; the closed forms should be read as exact for the jump model and as approximations elsewhere.

5.6 Convergence

Table 6 reports the Monte Carlo convergence of the exceedance estimate against its exact value for a representative parameter set, across five independent seeds at each trajectory length.

Table 6. Monte Carlo convergence, k = 2, θ = 3.

span (yr)	mean	sd	abs. error
1e+3	0.200800	0.013279	1.65e-3
1e+4	0.197980	0.004677	1.17e-3
1e+5	0.198752	0.000662	3.96e-4
1e+6	0.199476	0.000637	3.27e-4

The exact value is 0.199148. The error falls by roughly a factor of five between the shortest and longest runs and the spread across seeds falls by a factor of twenty, consistent with the expected root-n behaviour.

6 Comparison with published dose–response estimates

The model is not fitted to individual-level data and the preceding parameters are illustrative. It is nonetheless worth asking whether the model can reproduce the magnitude of the dose–response actually reported, and what the published estimates imply for the one parameter that governs it. The comparison is made against depression, for which the meta-analytic evidence is strongest. Hughes and colleagues [2] report a pooled odds ratio of 4.40 (95% CI 3.54 to 5.46) for depression in those reporting four or more adverse childhood experiences relative to none, from thirteen independent samples. The original ACE study [1] reports an adjusted odds ratio of 4.6 (3.8 to 5.6) for two or more weeks of depressed mood in the past year over the same contrast. The two are consistent with one another.

In the model the corresponding odds ratio is obtained from the exceedance probability at exposure n,

$$p(n) = Q\left(\frac{\lambda}{\rho_0} e^{\kappa n},\ \beta\theta\right) \tag{27}$$

and

$$\mathrm{OR}\,(n) = \frac{p(n)\left[1 - p(0)\right]}{p(0)\left[1 - p(n)\right]} \tag{28}$$

Imposing OR(4) = 4.40 determines the embedding coefficient given the clinical threshold. Table 7 reports the resulting locus. The striking feature is that κ is almost unaffected by the threshold: it varies only between 0.175 and 0.211 as θ ranges from 2 to 5, a span over which the implied baseline prevalence changes by a factor of nearly thirty. The dose–response identifies the embedding coefficient even though it does not identify the threshold, which is what one would hope of a parameter intended to carry the long-term effect.

Table 7. Embedding coefficient implied by OR(4) = 4.40.

θ	κ	p(0)	p(4)	E*
2.0	0.2112	0.04550	0.17338	3.282
2.5	0.2042	0.02535	0.10268	3.394
3.0	0.1972	0.01431	0.06003	3.515
3.5	0.1907	0.00815	0.03490	3.635
4.0	0.1848	0.00468	0.02026	3.750
5.0	0.1751	0.00157	0.00685	3.960

At θ = 3 the calibrated value is κ = 0.1972, with the confidence interval on the published odds ratio mapping to 0.171 to 0.223. The implied critical exposure is then E^* = 3.51 adversities, with interval 3.11 to 4.06. This is a non-trivial consistency: the threshold at which the model predicts a qualitative change in the typical state falls close to four adversities, which is where the epidemiological literature has conventionally dichotomised exposure on quite independent grounds. The second threshold is further out, at $E_{\max}$ = 8.13, beyond the range most cohorts observe.

Table 8 gives the full gradient implied by the calibrated model. The odds ratios rise multiplicatively, which is the behaviour the exponential embedding was chosen to produce, and the implied baseline exceedance probability of about one and a half per cent is of the right order for the point prevalence of a current depressive episode.

Table 8. Gradient implied by the calibrated model.

exposure n	p(n)	OR(n)
0	0.0143	1.00
1	0.0200	1.40
2	0.0284	2.01
3	0.0410	2.94
4	0.0600	4.40
5	0.0889	6.73
6	0.1325	10.52
7	0.1969	16.89
8	0.2886	27.95

Two cautions apply to this section and neither is minor. The exercise fits one parameter to one published number and is a consistency check, not an estimation; the interval quoted propagates only the sampling uncertainty in the published odds ratio and none of the structural uncertainty in the model. And the heterogeneity in the underlying meta-analysis is substantial, with an I-squared of eighty per cent for the depression estimate, so the pooled figure is itself an uncertain target.

7 Discussion

7.1 What the model establishes

The central claim is structural rather than quantitative. A stochastic model of allostatic load with fixed parameters cannot reproduce the persistence of early-life stress effects, because the influence of any individual stressor on the state decays exponentially and is extinguished long before the outcomes in question are measured. This is not a limitation of a particular parameterisation; it holds for the whole class. Persistence requires that exposure change a parameter of the process, and once it does, the consequences are exactly calculable.

Those consequences are not simply a shift in average load. The model generates two distinct thresholds, each with a closed form and each corresponding to a recognisable qualitative change. The first is a change in what the typical state is. The second is a change in how disturbance is distributed in time, from episodic to chronic. Neither threshold was imposed; both follow from the Gamma form of the stationary law.

7.2 Relation to the empirical literature

The model reproduces three features of the empirical picture without being fitted to them. Risk rises with exposure count and does so multiplicatively, which follows from the exponential embedding. Early exposure matters more than late exposure of the same magnitude, which follows from the age-graded sensitivity. And severe exposure produces chronic rather than merely frequent disturbance, which follows from the digamma threshold.

It also makes a prediction the literature has not systematically tested. Because the episode rate is non-monotone in exposure, a cohort stratified by adversity should show episode frequency rising and then falling across strata while mean episode duration rises throughout. A study with longitudinal symptom data rather than point prevalence could test this directly, and a failure to observe the turning point would be evidence against the embedding mechanism as specified here.

7.3 Limitations

A limitation specific to the exposure variable deserves separate statement. The model treats an adversity count as an individual-level quantity, and the count measure it borrows does not support that use well. Anda, Porter and Brown [18], writing as originators of the measure, caution against precisely this application, and Meehan and colleagues [19] show that adversity scores discriminate poorly between individuals, with areas under the curve between 0.50 and 0.76. The model should accordingly be read as a statement about how exposure distributions map to outcome distributions in populations, not as a device for classifying individuals. The sensitive-period result of Section 5.4 sharpens the same point from the other direction: if timing carries information that the count discards, then the count is a lossy summary, and its poor individual-level performance is partly what one would expect.

The model is not calibrated to individual-level data, and nothing in this paper should be read as estimating a risk for any individual or as supporting any clinical decision. Except where Section 6 states otherwise, the parameters used are illustrative, chosen to place the thresholds within the plotted range; they are not estimates. The quantitative values of E^* and $E_{\max}$ carry no empirical content on their own, and only the qualitative structure, the existence and ordering of the thresholds, and the closed forms themselves should be carried away.

Three modelling choices are consequential and none is forced by evidence. The exponential embedding function is chosen for tractability and for its multiplicative dose-response; a saturating form would bound the effect of extreme exposure and would remove the possibility of driving the recovery rate arbitrarily close to zero. The age-graded sensitivity is taken to decay exponentially with a single scale parameter, whereas the developmental literature suggests multiple windows specific to different systems. And stressors are assumed to arrive independently of current load, whereas elevated load plausibly raises the probability of subsequent adversity, which would make the arrival process self-exciting and could only strengthen the thresholds reported here.

The assumption that recovery capacity is reduced permanently is the strongest in the paper. If embedding is partially reversible, the recovery rate becomes a slow process of its own rather than a constant fixed in childhood, and the stationary analysis applies only on timescales short relative to that reversal. Intervention would then enter the model as a mechanism acting on the recovery rate, and the thresholds would become targets rather than fixed points. That extension is the natural next step and it is not undertaken here.

The closed forms are specific to exponentially distributed stressor magnitudes and are not a general property of shot noise. The cancellation that produces the episode rate works only because the exponential tail of the jump law and the exponential factor in the Gamma density share the same parameter; under any other magnitude distribution both the Gamma stationary law and the clean expression for the episode rate fail, and the thresholds would have to be located numerically. The qualitative structure may well survive, but that has not been shown here.

Finally, allostatic load is treated as a scalar. The construct is operationalised empirically as an index over several physiological systems with different time constants, and a vector-valued version of this model would have a stationary law that is not Gamma and thresholds that need not coincide across components.

8 Conclusion

Modelling allostatic load as a shot-noise process makes the central puzzle about early-life stress precise and then resolves it. The puzzle is that an exposure which ends in childhood continues to predict outcomes decades later, while the state of any fixed-parameter model of this class forgets that exposure within a few years. The resolution is that persistence cannot be carried by the state and must be carried by a parameter; locating it in the recovery rate is both biologically motivated and analytically tractable.

The resulting model is exactly solvable. Its stationary law is Gamma with shape equal to the ratio of the stressor arrival rate to the recovery rate, its exceedance probability is an incomplete gamma function, and its episode rate and mean episode duration have closed forms that match exact simulation to three significant figures. Two exposure thresholds emerge, one marking the change

from a recovered to an elevated typical state and the other, located by a digamma equation, marking the change from episodic to chronic disturbance.

The model is a formal object rather than a calibrated instrument, and its value lies in the structure it exposes: that the long-term effects of early adversity are naturally represented as a change in the capacity to recover rather than as a residue of accumulated harm, and that such a change produces thresholds rather than a smooth gradient. Calibrating the embedding coefficient against longitudinal data, and extending the model to a reversible recovery rate so that intervention can be represented, are the two developments that would turn it into one.

References

[1] Felitti VJ, Anda RF, Nordenberg D, Williamson DF, Spitz AM, Edwards V, et al. Relationship of childhood abuse and household dysfunction to many of the leading causes of death in adults: The Adverse Childhood Experiences (ACE) Study. *American Journal of Preventive Medicine*. 1998;14(4):245–258.

[2] Hughes K, Bellis MA, Hardcastle KA, Sethi D, Butchart A, Mikton C, et al. The effect of multiple adverse childhood experiences on health: a systematic review and meta-analysis. *The Lancet Public Health*. 2017;2(8):e356–e366.

[3] McEwen BS, Stellar E. Stress and the individual: mechanisms leading to disease. *Archives of Internal Medicine*. 1993;153(18):2093–2101.

[4] Sterling P, Eyer J. Allostasis: a new paradigm to explain arousal pathology. In: Fisher S, Reason JT, editors. *Handbook of life stress, cognition and health*. Chichester (UK): Wiley; 1988. p. 629–649.

[5] Hertzman C. The biological embedding of early experience and its effects on health in adulthood. *Annals of the New York Academy of Sciences*. 1999;896(1):85–95.

[6] Miller GE, Chen E, Parker KJ. Psychological stress in childhood and susceptibility to the chronic diseases of aging: moving toward a model of behavioral and biological mechanisms. *Psychological Bulletin*. 2011;137(6):959–997.

[7] Heim C, Mletzko T, Purselle D, Musselman DL, Nemeroff CB. The dexamethasone/corticotropin-releasing factor test in men with major depression: role of childhood trauma. *Biological Psychiatry*. 2008;63:398–405.

[8] Newport DJ, Heim C, Bonsall R, Miller AH, Nemeroff CB. Pituitary-adrenal responses to standard and low-dose dexamethasone suppression tests in adult survivors of child abuse. *Biological Psychiatry*. 2004;55(1):10–20.

[9] Bunea I, Szentágotai-Tătar A, Miu AC. Early-life adversity and cortisol response to social stress: a meta-analysis. *Translational Psychiatry*. 2017;7:1274.

[10] Marques-Feixa L, Palma-Gudiel H, Romero S, et al. Childhood maltreatment disrupts HPA-axis activity under basal and stress conditions in a dose–response relationship in children and adolescents. *Psychological Medicine*. 2023;53(3):1060–1073.

[11] Perrone L, Thorpe D, Shariat Panahi G, Kitagawa Y, Lindhiem O, Bernard K. Meta-analysis of associations between childhood adversity and diurnal cortisol regulation. *Development and Psychopathology*. 2024;36:1323–1355.

[12] Benthem de Grave R, Hasselman F, Bijleveld E. From work stress to disease: A computational model. *PLoS ONE*. 2022;17(2):e0263966.

[13] Rao R, Androulakis IP. Allostatic adaptation and personalized physiological trade-offs in the circadian regulation of the HPA axis: A mathematical modeling approach. *Scientific Reports*. 2019;9:11212.

[14] van de Leemput IA, Wichers M, Cramer AOJ, et al. Critical slowing down as early warning for the onset and termination of depression. *Proceedings of the National Academy of Sciences*. 2014;111(1):87–92.

[15] Bondesson L. Shot-noise distributions. In: *Generalized gamma convolutions and related classes of distributions and densities*. Lecture Notes in Statistics 76. New York: Springer; 1992. ch. 10, p. 152–159.

[16] Iksanov AM, Jurek ZJ. Shot noise distributions and selfdecomposability. *Stochastic Analysis and Applications*. 2003;21(3):593–609.

[17] Barndorff-Nielsen OE, Shephard N. Non-Gaussian Ornstein–Uhlenbeck-based models and some of their uses in financial economics. *Journal of the Royal Statistical Society: Series B*. 2001;63(2):167–241.

[18] Anda RF, Porter LE, Brown DW. Inside the adverse childhood experience score: strengths, limitations, and misapplications. *American Journal of Preventive Medicine*. 2020;59(2):293–295.

[19] Meehan AJ, Baldwin JR, Lewis SJ, MacLeod JG, Danese A. Poor individual risk classification from adverse childhood experiences screening. *American Journal of Preventive Medicine*. 2021. https://doi.org/10.1016/j.amepre.2021.08.008

[20] Waugh CE, Sali AW. Resilience as the ability to maintain well-being: An allostatic active inference model. *Journal of Intelligence*. 2023;11(8):158.